Floral Induction in Arabidopsis by FLOWERING LOCUS T Requires Direct Repression of *BLADE-ON-PETIOLE* Genes by the Homeodomain Protein PENNYWISE[1][OPEN]

Fernando Andrés, Maida Romera-Branchat, Rafael Martínez-Gallegos, Vipul Patel, Korbinian Schneeberger, Seonghoe Jang[2], Janine Altmüller, Peter Nürnberg, and George Coupland*

Max Planck Institute for Plant Breeding Research, D–50829 Cologne, Germany (F.A., M.R.-B., R.M.-G., V.P., K.S., S.J., G.C.); and Cologne Center for Genomics (J.A., P.N.), Institute of Human Genetics (J.A.), Center for Molecular Medicine Cologne (P.N.), and Cologne Excellence Cluster on Cellular Stress Responses in Aging-Associated Diseases (P.N.), University of Cologne, 50931 Cologne, Germany

ORCID IDs: 0000-0003-4736-8876 (F.A.); 0000-0002-6685-5066 (M.R.-B.); 0000-0003-0012-5033 (R.M.-G.); 0000-0001-5018-3480 (S.J.); 0000-0001-6988-4172 (G.C.).

Flowers form on the flanks of the shoot apical meristem (SAM) in response to environmental and endogenous cues. In Arabidopsis (*Arabidopsis thaliana*), the photoperiodic pathway acts through *FLOWERING LOCUS T* (*FT*) to promote floral induction in response to day length. A complex between FT and the basic leucine-zipper transcription factor FD is proposed to form in the SAM, leading to activation of *APETALA1* and *LEAFY* and thereby promoting floral meristem identity. We identified mutations that suppress FT function and recovered a new allele of the homeodomain transcription factor PENNYWISE (PNY). Genetic and molecular analyses showed that ectopic expression of *BLADE-ON-PETIOLE1* (*BOP1*) and *BOP2*, which encode transcriptional coactivators, in the SAM during vegetative development, confers the late flowering of *pny* mutants. In wild-type plants, *BOP1* and *BOP2* are expressed in lateral organs close to boundaries of the SAM, whereas in *pny* mutants, their expression occurs in the SAM. This ectopic expression lowers *FD* mRNA levels, reducing responsiveness to FT and impairing activation of *APETALA1* and *LEAFY*. We show that PNY binds to the promoters of *BOP1* and *BOP2*, repressing their transcription. These results demonstrate a direct role for PNY in defining the spatial expression patterns of boundary genes and the significance of this process for floral induction by FT.

Plants produce new organs from a population of pluripotent cells in meristems whose function is related to stem cells in animals. Meristems are located at different positions of the plant body and give rise to different organs. The shoot apical meristem (SAM) produces leaves and flowers at the tips of stems, whereas the axillary meristems give rise to lateral structures (Bowman and Eshed, 2000). By reprogramming these pluripotent cells at the meristems, plants can readily modify their development in response to changes in environmental conditions.

Flowers develop from floral meristems (FMs) that are formed on the flanks (floral primordium) of the SAM in response to environmental and endogenous cues (Pidkowich et al., 1999). Major environmental signals are the seasonal fluctuations in temperature and day length that are used by plants to anticipate optimal conditions for reproduction. Changes in temperature and day length are integrated into flowering-signaling networks by the thermosensory and vernalization/autonomous pathways and the photoperiodic pathway, respectively (Martinez-Zapater and Somerville, 1990; Lee and Amasino, 1995; Valverde et al., 2004; Andrés and Coupland, 2012). On the other hand, the plant hormone GA and the age of the plant constitute the internal signals affecting flowering in many plant species (Wilson et al., 1992; Fowler et al., 1999; Yu et al., 2012). *FLOWERING LOCUS T* (*FT*) is a key component of the photoperiodic pathway. *FT* encodes a small globular protein that shares high homology with mammalian phosphatidylethanolamine-binding proteins/Raf-1 kinase inhibitory protein (Kardailsky et al., 1999; Kobayashi et al., 1999; Nakamura

et al., 2014; Romera-Branchat et al., 2014). In Arabidopsis (*Arabidopsis thaliana*), *FT* is induced by long days (LDs) and has been placed at the core of the photoperiodic pathway, downstream of the *GIGANTEA* and *CONSTANS* genes (Suárez-López et al., 2001; Valverde et al., 2004; Yoo et al., 2005). *FT* mRNA is expressed specifically in the companion cells of the phloem, and its protein moves systemically to the shoot apex through the phloem sieve elements (Corbesier et al., 2007; Jaeger and Wigge, 2007; Mathieu et al., 2007; Tamaki et al., 2007). According to recent studies in *Cucurbita moschata* and Arabidopsis, FT protein is unloaded into the surrounding shoot meristem tissue from the terminal phloem (Yoo et al., 2013). Once FT is unloaded into the shoot meristem, it is thought to physically interact with two basic leucine-zipper (bZIP) transcription factors called FD and FD PARALOG (FDP), which are expressed in this tissue (Abe et al., 2005; Wigge et al., 2005). However, recent work in rice (*Oryza sativa*) suggested that this interaction is not direct and is mediated by 14-3-3 proteins (Taoka et al., 2011). Consistent with this model, the loss of function of *FD* and *FDP* strongly suppresses the early flowering of transgenic plants overexpressing *FT* (Abe et al., 2005; Wigge et al., 2005; Jaeger et al., 2013). In Arabidopsis, the FT-FD complex is believed to induce the transcription of genes encoding several floral-promoting proteins, such as the MADS-box transcription factors SUPPRESSOR OF OVEREXPRESSION OF CONSTANS1 (SOC1) and FRUITFULL (FUL), which accelerate flowering, as well as APETALA1 (AP1), also a MADS-box transcription factor, and LEAFY (LFY), which promote FM identity (Schmid et al., 2003; Teper-Bamnolker and Samach, 2005; Wigge et al., 2005; Corbesier et al., 2007). Indeed, the FT-FD complex directly binds to the promoter of *AP1*, whose expression at the floral primordia is associated with FM formation (Wigge et al., 2005). Therefore the FT-FD complex is predicted to be active in the incipient floral primordia to induce the expression of *AP1* and promote flowering. In addition to these genes, the FT-FD complex also promotes the transcription of the family genes encoding the SQUAMOSA BINDING PROTEIN LIKE (SPL) transcription factors. Recent studies using chromatin immunoprecipitation (ChIP) assays showed that *SPL3*, *SPL4*, and *SPL5* loci are bound by FD, which transcriptionally regulates these genes (Jung et al., 2012). In turn, SPL proteins control the expression of *FUL*, *LFY*, and *AP1* genes by directly binding to their promoters (Wang et al., 2009; Yamaguchi et al., 2009). These data reflect the high degree of complexity implicit to the genetic networks controlling floral induction in the SAM.

The three-amino acid-loop-extension (TALE) homeodomain superclass comprises transcription factors involved in the SAM function. The BEL1-like homeodomain (BELL) and the KNOTTED-like homeodomain (KNOX) are TALE proteins that share similar structure and function (Hamant and Pautot, 2010; Hay and Tsiantis, 2010; Arnaud and Pautot, 2014). Members of the two families can form heterodimers to regulate various developmental processes. The *BELL* family comprises 13 members (Smith et al., 2004). *PENNYWISE* (*PNY*), also known as *BELLRINGER*, *REPLUMLESS* (*RPL*), *VAAMANA*, or *LARSON*, encodes a BELL protein that plays roles in organ patterning by affecting internode length, phyllotaxis, and fruit replum development (Byrne et al., 2003; Roeder et al., 2003; Smith and Hake, 2003). In fruits, *PNY* is required for the replum formation, where it acts as a transcriptional repressor of *SHATTERPROOF* (*SHP*) MADS-box genes. The repressive activity of *PNY* restricts *SHP* gene expression to the valve margin domain. In the absence of a functional *PNY* (in *rpl* mutants), *SHP* genes are ectopically expressed, and the replum cells take on valve margin fates (Roeder et al., 2003). *PNY* mutants also display dramatic defects in inflorescence development (Smith and Hake, 2003; Bao et al., 2004). Interestingly, these defects are corrected by the lack of *KNOTTED*-like from *Arabidopsis thaliana6* (*KNAT6*) and *KNAT2*, two related *KNOX* genes. In the *pny* mutant, *KNAT2* and *KNAT6* expression domains are enlarged, indicating that PNY regulates inflorescence development at least partially by limiting their spatial pattern of expression (Ragni et al., 2008). These data suggest that a major molecular function of PNY is to maintain the spatial expression of organ patterning genes restricted to specific domains.

Recent studies elucidated that *PNY* is also involved in the acquisition of competence to respond to floral inductive signals. In these studies, it was shown that simultaneous loss of function of *PNY* and its paralog *POUND-FOOLISH* (*PNF*) completely blocks the floral transition. Indeed, the double mutant *pny pnf* is not able to undergo the floral transition, even under LD conditions (Smith et al., 2004). Moreover, overexpression of *FT* from the constitutive *Cauliflower mosaic virus 35S* promoter barely activates flowering of the *pny pnf* double mutant (Kanrar et al., 2008). At the molecular level, the concurrent loss of function of *PNY* and *PNF* affects the ability of FT to activate the transcription of *AP1*, *LFY*, and probably *SPLs* (Lal et al., 2011). Therefore, *PNY* has somehow been integrated into the *FT*-signaling pathway. However, the genetic and molecular mechanism underlying the effect on PNY on the FT flowering pathway remains unknown.

Here, we show that *PNY* operates in the FT-signaling pathway by restricting the spatial pattern of expression of *BLADE-ON-PETIOLE1* (*BOP1*) and *BOP2* genes in the SAM. PNY directly binds to *BOP1* and *BOP2*, which encode two BTB (for Broad-complex, Tramtrack, Bric-à-brac)-ankyrin transcriptional coactivators, which function at lateral organ boundaries in the determination of leaf, flower, inflorescence, and root nodule architecture (Ha et al., 2004, 2007; Hepworth et al., 2005; Norberg et al., 2005; Karim et al., 2009; Xu et al., 2010; Couzigou et al., 2012; Khan et al., 2012b, 2014). We found that *BOP1* and *BOP2* are also involved in flowering-time regulation by repressing the expression of *FD* in the shoot meristem. These data indicate that PNY has an unexpected function during plant development in regulating the pattern of expression of

flowering-time genes in the shoot meristem by repressing *BOP1/2* gene transcription.

RESULTS

A Sensitized Forward Genetic Screen followed by Fast Isogenic Mapping Identifies *PNY* as a Regulator of the FT-Signaling Pathway

A sensitized genetic screen was designed to identify genes affecting the ability of FT to activate flowering. In the double mutant *ft-10 tsf-1*, which carries null mutations in *FT* and its closest homolog *TWIN SISTER OF FLOWERING LOCUS T* (*TSF*), the floral promotion activity of FT is abolished, causing late flowering and insensitivity to photoperiod (Yamaguchi et al., 2005; Jang et al., 2009). FT function in *ft-10 tsf-1* can be restored using the transgene p*GAS1::FT* (GALACTOL SYNTHASE1 [GAS1] promoter fused to FT), which is active only in phloem companion cells of the minor veins (Jang et al., 2009). Thus, p*GAS1::FT ft-10 tsf-1* plants show early flowering compared with *ft-10 tsf-1* double mutants under LDs and short days (SDs). These plants were used to screen for mutations that suppress promotion of flowering by FT. Seeds of p*GAS1::FT ft-10 tsf-1* were mutagenized with ethyl methanesulfonate (EMS), and late-flowering plants were screened in the M2 generation under SD. Recovered mutants are hereafter called *late flowering in pGAS::FT ft-10 tsf-1* (*lgf*). Early flowering of p*GAS::FT ft-10 tsf-1* plants grown under SD is entirely dependent on movement of FT from the leaves to the SAM, so *lgf* mutations were

expected to define genes required for FT function or transport. Around 35,000 M2 plants were screened, and several *lgf* mutants were selected (Supplemental Fig. S1). The *lgf58* mutation most strongly suppressed the early flowering conferred by misexpression of FT (Fig. 1; Supplemental Fig. S1). This mutant also showed other phenotypic abnormalities, such as short stature and lanceolate leaves (Supplemental Fig. S1).

The fast isogenic mapping approach was used to identify the *lgf58* mutation (Hartwig et al., 2012; Schneeberger, 2014). A mapping population was created by backcrossing *lgf58* to p*GAS::FT ft-10 tsf-1* and self fertilizing the resulting F1 plants. A total of 566 BC1F2 plants were grown, and 174 of them exhibited the late-flowering phenotype of *lgf58* (an approximate ratio of 3:1), suggesting that a single recessive mutation was responsible for the effect. To construct the pool, an individual leaf from each of the 174 plants showing the mutant phenotype was collected. Genomic DNA extracted from the pooled material and the progenitor p*GAS::FT ft-10 tsf-1* were sequenced using Illumina technology. By applying SHOREmap (Schneeberger et al., 2009b; Sun and Schneeberger, 2015), candidate loci, at which mutant alleles were strongly overrepresented in the pool, were identified on the top arm of chromosome 5 (Fig. 1; Supplemental Fig. S2; for more details, see also "Materials and Methods"). Three loci were selected as high-confidence candidates because they carried a nonsynonymous mutation and showed an allele frequency equal to 1.0 and a quality score equal to 40 (Supplemental Table S1; "Materials and Methods"). Among the highest probability candidates,
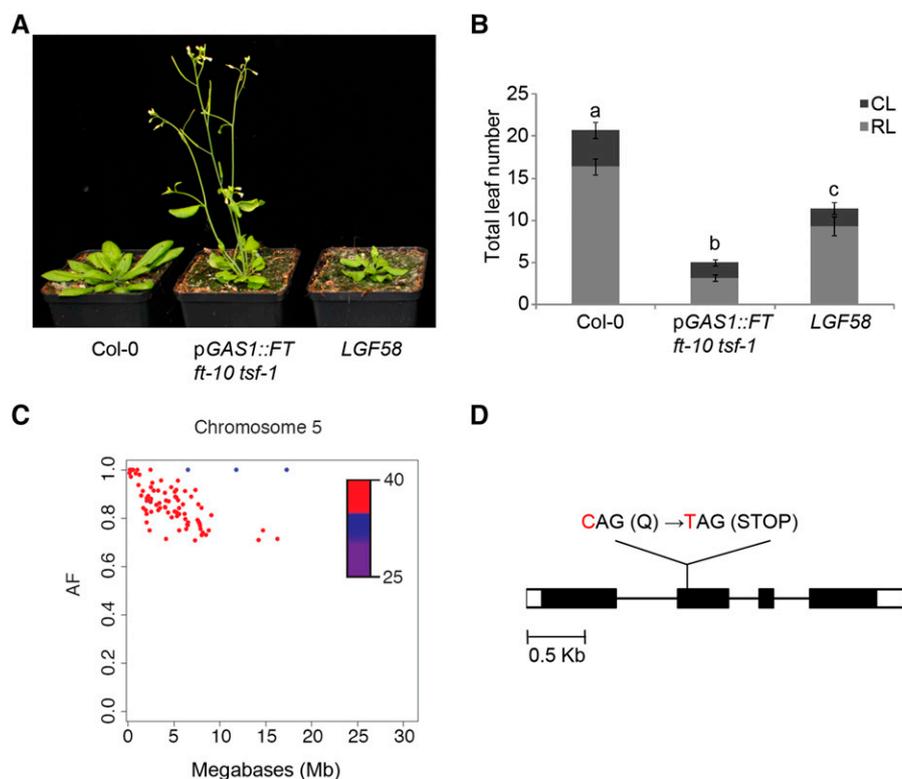

Figure 1. Identification and cloning of a functional suppressor of FT. Phenotypic comparison between *lgf58*, p*GAS1::FT ft-10 tsf-1* and Columbia-0 (Col-0) wild-type plants (A) and their flowering time under LD ($n = 10$; B). CL, Cauline leaves; RL, rosette leaves. Letters shared in common between the genotypes indicate no significant difference (Student's *t* test, $P < 0.05$). C, Graphic showing the allelic frequency estimations at EMS-induced mutations (AF; *y* axis) across chromosome 5 (Mb; *x* axis) of *lgf58*. AFs were calculated by dividing the number of reads supporting the mutant allele by the number of all reads aligning to a given marker. The color code indicates the resequencing consensus (SHORE) score. EMS mutations showing a SHORE score higher than 25 were selected. AFs in chromosome 5 were higher compared with other regions in the genome (see also Supplemental Fig. S2). D, Scheme of the *PNY* locus showing the position of the mutation and the sequence change found in *lgf58*.

the gene *AT5G02030* contained a mutation in the second exon predicted to produce a premature stop codon (Fig. 1; Supplemental Table S1). *AT5G02030* encodes the BELL protein PNY. Mutations in *PNY* cause defects in plant architecture, abnormalities in the fruit replum, and late flowering (Byrne et al., 2003; Roeder et al., 2003; Smith and Hake, 2003; Bao et al., 2004; Smith et al., 2004). Double mutants containing mutations in *PNY* and its paralog *PNF* fail to undergo the transition from vegetative to reproductive phase, even in the presence of high levels of *FT* mRNA expressed from the *35S* promoter (Kanrar et al., 2008). Similar phenotypes were also observed in *lgf58* (Fig. 1; Supplemental Fig. S1) and in Col-0 plants carrying the newly isolated mutant allele of *PNY* (hereafter called *pny-58*) segregated away from p*GAS*::*FT ft-10 tsf-1* (Supplemental Fig. S3). Previously, *pny pnf* double mutants were proposed to be blocked in the floral transition due to impairment of the ability of FT to activate the transcription of downstream target genes, such as *AP1*. In agreement with this idea, the mRNA levels of *AP1*, *LFY*, and *SPL4*, which are transcriptionally activated downstream of FT, were dramatically reduced in the *lgf58* mutant compared with p*GAS*::*FT ft-10 tsf-1*. However, as also described earlier for *pny pnf* double mutants, *SOC1* mRNA expression was unaltered in *lgf58* (Supplemental Fig. S1; Kanrar et al., 2008). Col-0 plants carrying the *pny-58* mutant allele grown under LD also showed late flowering compared with wild-type plants and were more extreme than the previously reported mutant allele *pny-40126* (Smith and Hake, 2003; Ragni et al., 2008; Supplemental Fig. S3). This delay in flowering was corrected by introducing a transgenic copy of the wild-type genomic *PNY* locus into the mutant plants (p*PNY*::*Venus*:*PNY pny-58*), confirming that the mutation *pny-58* was responsible for the late-flowering phenotype (Supplemental Fig. S4). Moreover, the early flowering of p*GAS*::*FT ft-10 tsf-1* was also reduced by combining it with the mutant allele *pny-40126*, but the effect on flowering was less severe than for *lgf58* (Supplemental Fig. S4). These results demonstrate that the sensitized suppressor screen identified a novel allele of *PNY* that causes a stronger delay in flowering than those previously described, and which strongly reduces the ability of *FT* to activate flowering.

Regulation of *PNY* during Photoperiodic Induction of Flowering

Loss of *PNY* function reduced the capacity of FT to activate flowering in response to inductive LD photoperiods or in transgenic p*GAS*::*FT* plants expressing higher levels of *FT* mRNA. *PNY* mRNA is expressed in the SAM (Smith and Hake, 2003), but whether it is regulated in response to changes in day length is unknown. *PNY* mRNA distribution was analyzed by in situ hybridization in different environments (Fig. 2). Under SD, *PNY* mRNA was expressed in the central zone of the SAM and excluded from the leaf boundaries
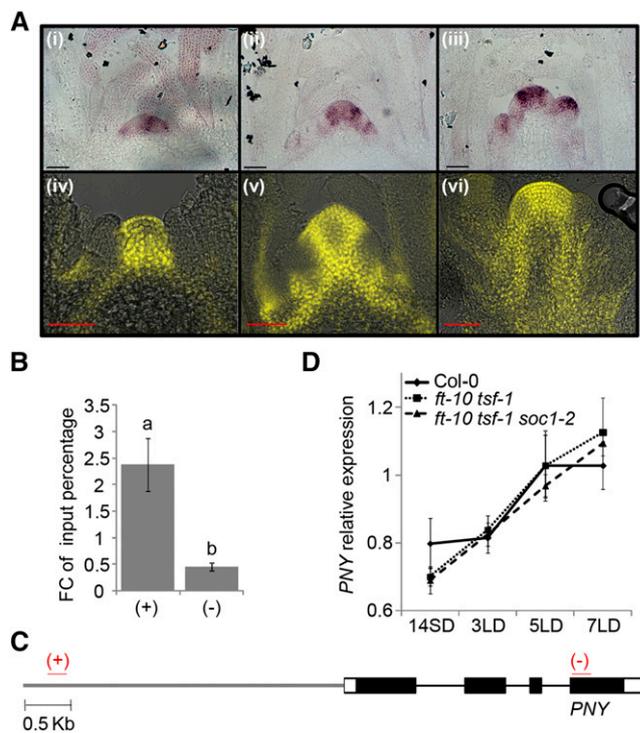
Figure 2. Pattern of expression of *PNY* during photoperiod flowering. A, *PNY* mRNA (i–iii) and protein accumulation (iv–vi). Plants were grown for 14 d under SD (i and iv; vegetative stage) and then shifted to LD for 3 (ii and v; floral transition) and 5 additional days (iii and vi; flower development). Scale bars = 50 μM. B, ChIP-quantitative PCR (qPCR) showing binding of SOC1:GFP on *PNY* promoter. The *y* axis represents the fold change (FC) of enrichment (percentage of input) between the qPCR results using positive primers (flanking a CArG-box motif) and the negative ones (flanking the coding sequence of PNY). Letters shared in common between the genotypes indicate no significant difference (Student's *t* test, $P < 0.05$). C, Localization of the primers used for ChIP-qPCR of SOC1:GFP on the *PNY* promoter. Region (+) contains a CArG-box cis-motif, which was enriched after immunoprecipitation of SOC1:GFP. Region (−) was used as a negative control. D, Study of the *PNY* expression in plants shifted from SDs to LDs. Plants were grown for 2 weeks under SDs and then shifted to LDs for 3, 5, and 7 additional days. RNA was extracted from dissected shoot apices. Error bars indicate SD.

(Fig. 2). After transferring plants to LD, *PNY* mRNA was detected more broadly, but was still not detected in leaf boundaries, nor in floral primordia. The pattern of PNY protein expression was also tested by constructing p*PNY*::*Venus*:*PNY pny-40126* plants (Fig. 2; Supplemental Fig. S5). The transgene complemented the defects of the *pny-4026* mutant. By confocal microscopy, *Venus*:*PNY* was detected in the same domains shown by in situ hybridization to express *PNY* mRNA in the shoot meristem (Fig. 2). Similarly, its pattern of expression broadened during photoperiodic induction of flowering, and was excluded from leaf boundaries and floral primordia (Fig. 2). Therefore, expression of *PNY* mRNA and its translated product is increased by photoperiod in specific domains of the apex.

SOC1 is an important mediator of the FT-signaling pathway, and its mRNA expression pattern in the SAM

overlaps with that of *PNY* (Jang et al., 2009; Torti et al., 2012). A recent genome-wide study identified the *PNY* promoter as a direct target of SOC1 (Immink et al., 2012). Therefore, binding of SOC1 to the *PNY* locus was tested directly by ChIP-qPCR. In this way, binding of SOC1 to the *PNY* promoter was confirmed. SOC1:GFP bound to the *PNY* promoter at approximately 3,400 bp from its start codon ATG, in a region containing a putative CArG box. This position was very close to the observed binding peak of SOC1 by ChIP sequencing (Immink et al., 2012). No binding of SOC1:GFP was found in a region comprising the fourth exon of *PNY*, which was used as a negative control (Fig. 2). These data suggest that SOC1 might contribute to photoperiodic induction of *PNY* during flowering. Whether *PNY* expression was reduced by mutations in *FT*, *TSF*, or *SOC1* was also tested. However, no differences in *PNY* mRNA levels were detected in the *ft-10 tsf-1*, *ft-10 tsf-1 soc1-2*, and *soc1-2* mutants compared with Col-0 during the floral transition (Fig. 2; Supplemental Fig. S6). These results suggested that *PNY* expression is increased by exposure to LDs, and that SOC1 might contribute to this, although at the times tested, no detectable difference in *PNY* expression could be associated with the loss of function of *SOC1*, *FT*, or *TSF* by reverse transcription (RT)-qPCR.

Suppression of FT Function by *pny* Is Caused by Ectopic Expression of *BOP* Genes

Mutations in *PNY* and other TALE transcription factors, such as *BREVIPEDICELLUS* (*BP*), impair Arabidopsis architecture, particularly shortening internodes and altering silique position and orientation (Byrne et al., 2003; Roeder et al., 2003; Smith and Hake, 2003). These defects in plant architecture in *pny* mutants are associated with broader expression of *BOP* genes in the inflorescence stem and pedicels and are suppressed in *pny bop1 bop2* triple mutants (Khan et al., 2012b). The role of *BOP* genes in the late flowering of *pny* mutants has not been examined, so we tested whether this aspect of the *pny-58* phenotype was due to an increase of *BOP* gene expression in the SAM prior to floral induction. In 7-d-old plants grown under LDs, *BOP1* and *BOP2* mRNA levels were higher in *pny-58* mutants compared with the wild type, as tested by RT-qPCR (Fig. 3). Similarly, these genes were more highly expressed in *lgf58* plants than in pGAS::*FT ft-10 tsf-1* (Fig. 3). In situ hybridization experiments detected broader expression of *BOP2* in the SAM of vegetative 7-d-old *pny-58* plants than in Col-0 (Fig. 3; Supplemental Fig. S7) and in 10-d-old plants that were undergoing the floral transition (Supplemental Fig. S7). To test whether this increase in *BOP1/2* expression during vegetative development contributed to the late flowering of *pny-58* mutants, the *pny-58 bop1-3 bop2-1* triple mutant was constructed. These plants flowered much earlier than *pny-58* at a similar time to *bop1-3 bop2-1*, which were slightly earlier flowering than Col-0 (Supplemental Fig.
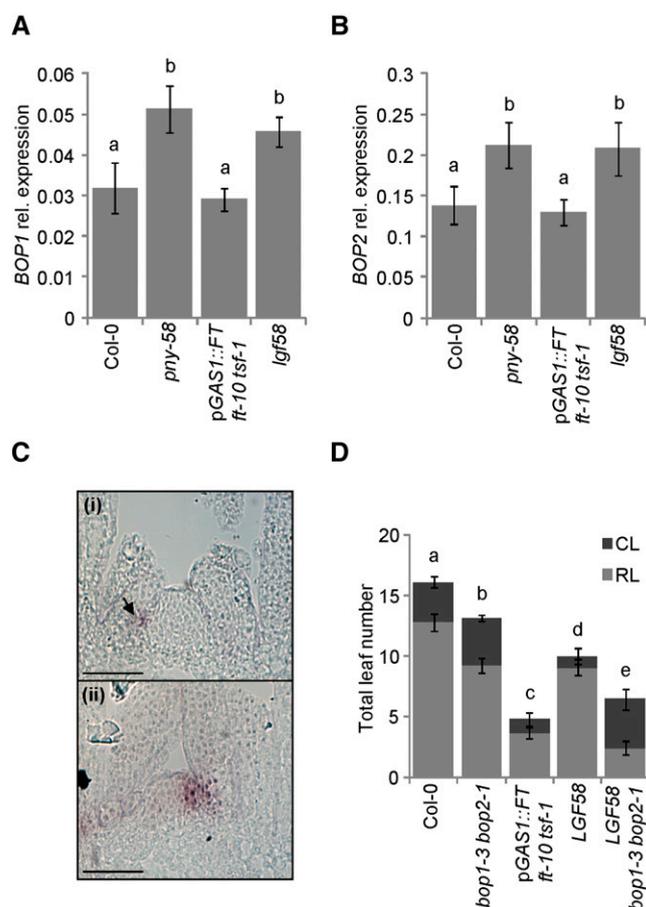
Figure 3. *BOP1/2* genes are important for flowering regulation mediated by PNY. Expression of *BOP1* (A) and *BOP2* (B) of shoot apices dissected from plants grown under LDs for 7 d. Letters shared in common between the genotypes indicate no significant difference (Student's *t* test, *P* < 0.05). C, In situ hybridizations with *BOP2* probe in shoot meristems of Col-0 (i) and *pny-58* (ii). Plants were grown for 7 LDs and stayed at the vegetative stage. Expression of *BOP2* in Col-0 plants was observed at the boundaries between leaves and the SAM (black arrow). Scale bars = 50 μM. D, Flowering time of the *BOP1/2* and *PNY* mutant combinations grown under LDs. CL, Cauline leaves; RL, rosette leaves. Error bars in A, B, and D indicate SD.

S7). Therefore, BOP1 and BOP2 are required for the late flowering of *pny-58* mutants. Similarly, introduction of *bop1-3 bop2-1* into the pGAS1::*FT pny-58* (*lgf58*) line restored flowering to a similar time to pGAS1::*FT ft-10 tsf-1* (Fig. 3; Supplemental Fig. S7), but the pGAS1::*FT bop1-3 bop2-1 pny-58* line (*lgf58 bop1 bop2*) produced a higher number of cauline leaves than pGAS1::*FT ft-10 tsf-1*, causing a slightly increased number of total leaves. This increased number of cauline leaves could be caused by the down-regulation of *LFY*, because *lfy* mutants produce more cauline leaves (Weigel et al., 1992), and *BOP1/2* promote *LFY* expression in the meristem (Karim et al., 2009). Thus, the levels of *LFY* mRNA in *bop1 bop2* at different developmental stages was quantified by RT-qPCR. Compared with the wild type, the expression of *LFY* in the *bop1 bop2* double
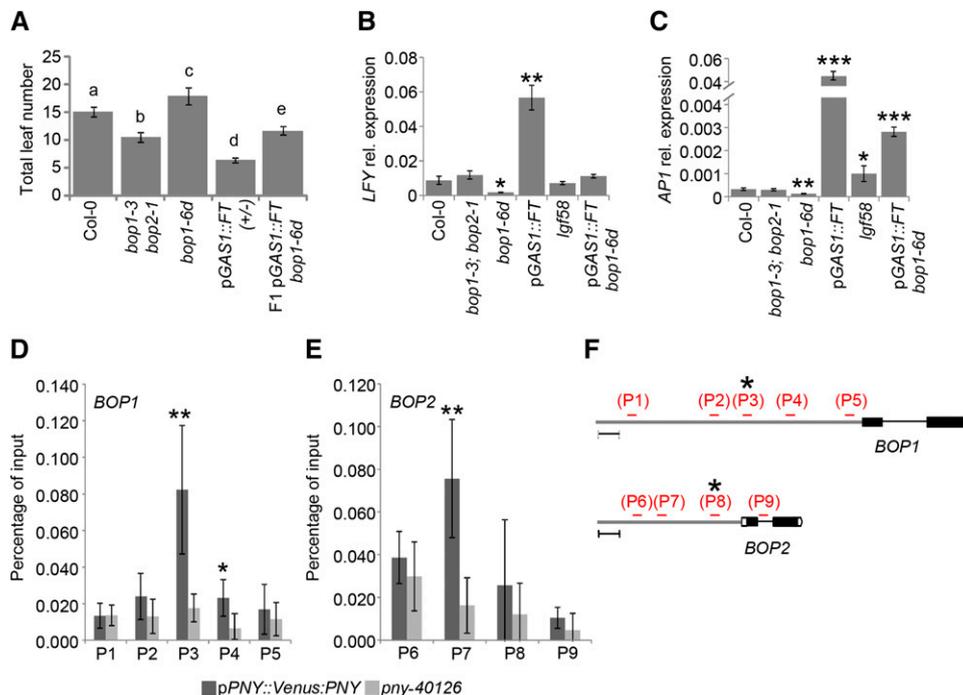
Figure 4. *BOP1/2* genes interfere with FT function and are directly bound by PNY. A, Flowering time of plants misexpressing *BOP* genes in the presence of high levels of *FT*. Letters shared in common between the genotypes indicate no significant difference (Student's *t* test, $P < 0.05$). B, Expression of *LFY* of dissected shoot apices of plants grown for 7 LDs. Asterisks indicate statistical differences between Col-0 and other genotypes (Student's *t* test; **, $P = 0.0004$; *, $P = 0.006$). C, Expression of *AP1* of dissected shoot apices of plants grown for 7 LDs. Asterisks indicate statistical differences between Col-0 and other genotypes (Student's *t* test; ***, $P = 0.001$; **, $P = 0.006$; *, $P = 0.03$). ChIP-qPCR of PNY on the promoters of *BOP1* (D) and *BOP2* (E). *x* axis indicates the primers used for its qPCR. Asterisks indicate statistical differences between p*PNY*::*Venus*:*PNY* and *pny-40126* (Student's *t* test; **, $P = 0.0001$; *, $P = 0.02$). F, Localization of the primers used for the ChIP-qPCR experiment on the *BOP1* (top scheme) and *BOP2* (bottom scheme) loci. *, AP1 binding genomic regions according to Kaufmann et al. (2010). Scale bars = 0.5 kb. Error bars in A to E indicate SD.

mutant was slightly increased during vegetative development (7–10 LDs) but reduced at the reproductive stage (17 LDs; Fig. 6).

Taken together these data support the hypothesis that late flowering of *pny-58* mutants is due to higher and ectopic expression of *BOP1/2* in the vegetative apex.

Since mutations in *PNY* suppress the capacity of FT to induce flowering, *BOP1/2* up-regulation should also delay the floral transition promoted by this protein. To explore this further, a dominant activation tagging allele of *BOP1* (*bop1-6D*) was used (Norberg et al., 2005). The *bop1-6D* mutants flowered later than Col-0 (Fig. 4). To test whether this occurs through the FT floral-promoting pathway, the double transgenic p*GAS1*::*FT bop1-6D* was constructed. Flowering time experiments demonstrated that *bop1-6D* delayed flowering of p*GAS1*::*FT* (Fig. 4). This result supports the idea that ectopic *BOP* expression impairs activity of the FT-signaling pathway. Indeed, the expression of *LFY* and *AP1*, which is activated in the SAM downstream of FT (Schmid et al., 2003; Moon et al., 2005), was dramatically reduced by overexpression of *BOP1* (Fig. 4).

These data together indicate that the repression of *BOP* genes in the shoot meristem by *PNY* is required for FT to efficiently promote the floral transition.

### PNY Represses *BOP1* and *BOP2* Transcription by Directly Binding to Their Promoters

The increase of *BOP1* and *BOP2* expression in *pny-58* mutants suggested that PNY might directly bind to the promoters of these genes. This possibility is further supported by proteomics analysis, which detected PNY and AP1 in the same transcriptional complex (Smaczniak et al., 2012), and by ChIP sequencing, which identified *BOP1* and *BOP2* as putative direct targets of AP1 (Kaufmann et al., 2010). Whether PNY binds to the same *BOP1/2* promoter regions as AP1 was therefore tested. ChIP-qPCR was performed on chromatin extracted from inflorescences of p*PNY*::*Venus*:*PNY* transgenic plants. The chromatin was immunoprecipitated using a GFP antibody, which detects Venus:PNY on western blots (Supplemental Fig. S7), followed by qPCR with combinations of primers spanning regions of the *BOP1* and *BOP2* promoters. Regions of the *TARGET OF EAT1*

(*TOE1*) and *LFY* promoters, which were shown to be directly bound by the AP1/PNY complex (Smaczniak et al., 2012), were used as positive controls. As expected, Venus:PNY bound to the *TOE1* and *LFY* loci within the same region that was reported for AP1 (Supplemental Fig. S7; Kaufmann et al., 2010). The binding of Venus:PNY to *BOP1* and *BOP2* was then tested. Venus:PNY bound to the *BOP1* promoter at two different positions (P3 and P4). One of these positions (P3) was the same as that reported for AP1 (Fig. 4; Kaufmann et al., 2010). An enrichment of chromatin immunoprecipitated by Venus:PNY was also detected within the *BOP2* promoter. In this case, the enrichment was found in a region located around 1 kb upstream of the one predicted for AP1 (Fig. 4). Notably, some potential PNY binding sites within these genomic regions were identified. For example, the P3 genomic region contains a core motif (ATGGAT) reported as a binding site for BEL1-LIKE HOMEODOMAIN (BLH1; Staneloni et al., 2009). Within the region P7, the two motifs AAATTACCA and AATTATCCT, which are similar to those previously identified as binding sites of BELLRINGER (BLR) in the *AGAMOUS* intronic region (AAATTAAAT, AAAT-TAGTC, and ACTAATTT; Bao et al., 2004; Smaczniak et al., 2012), were also found. However, only shorter versions of these motifs (AATTAT, AATTT, and AAATT) were identified within the P4 genomic region.

Collectively, these data indicate that PNY directly binds and represses the expression of *BOP1/2*.

Loss of *PNY* Function and *BOP* Overexpression Reduce the mRNA of FD, a Component of the FT-Signaling Pathway, in the Shoot Meristem

PNY loss of function caused a strong reduction in the expression of several genes, such as *SPLs*, *LFY*, and *AP1*, that are expressed at the apex during flowering downstream of FT (Supplemental Fig. S1). These results were in agreement with previous reports on *pny pnf* double mutants (Smith et al., 2004; Kanrar et al., 2008). However, the molecular mechanisms that cause the reduction of expression of these genes and a delay in flowering in *pny* mutants are not clear. FD directly interacts with FT (Abe et al., 2005; Moon et al., 2005), and mutations in *FD* and *PNY* were found to delay flowering of p*GAS*::*FT* transgenic plants to a similar extent (Supplemental Fig. S8), suggesting that they might influence the FT-signaling pathway at common positions. Furthermore, analysis of the mRNAs of *SPLs*, *LFY*, and *AP1* by RT-qPCR showed that the *fd-3* mutation suppressed the expression of these genes in a p*GAS1*::*FT* background to a similar extent as *pny-58* (Supplemental Fig. S8). These observations suggested that mutations in *PNY* might affect the FT-signaling pathway by reducing *FD* expression to impair photoperiodic floral induction by FT. To test this possibility, the expression of *FD* mRNA in *pny* mutants was analyzed. *FD* mRNA level was tested by RT-qPCR and was reduced in shoot apices of *pny-58* and *pny-40126* mutants compared with Col-0 wild-type plants (Fig. 5). Because *PNY* regulates
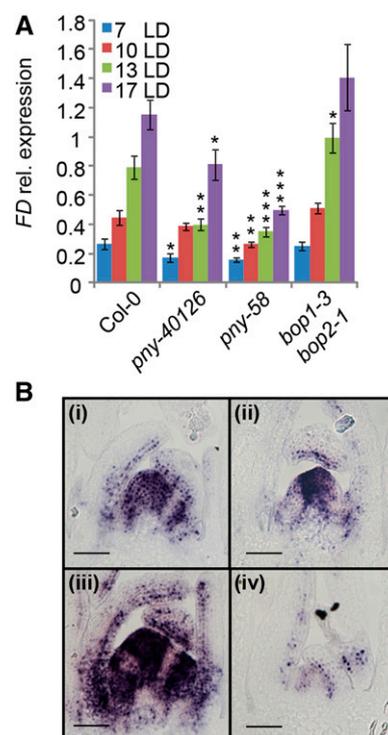

Figure 5. *BOP1/2* genes regulate the pattern of expression of *FD*. A, *FD* expression levels in different plants misexpressing *BOP1/2* and *PNY*. RNA was extracted from shoot apices of plants grown during 7 LDs (vegetative stage), 10 to 13 LDs (floral transition), and 17 LDs (reproductive stage). Asterisks indicate statistical differences between Col-0 and other genotypes (Student's *t* test; ***, *P* = 0.05; **, *P* = 0.01; *, *P* = 0.001). B, In situ hybridization of plants grown for 10 LDs showing the expression pattern of *FD* in Col-0 (i), *pny-58* (ii), *bop1-3 bop2-1* (iii), and *bop1-6D* (iv). Bar = 50 μM. Error bars in A to C indicate SD.

flowering through the transcriptional repression of *BOP* genes, the effect of *bop* mutations on *FD* mRNA level was tested. *FD mRNA* was slightly higher in *bop1-3 bop2-1* double mutants compared with Col-0 (Fig. 5). Moreover, in situ hybridization experiments showed that the *FD* mRNA was reduced in the meristem-leaf boundaries of the *pny-58* (Fig. 5). That this was due to ectopic expression of *BOP* genes was supported by the dramatic reduction in *FD* expression observed in meristems of *bop1-6D* (Fig. 5). By contrast, *FD* mRNA appeared slightly increased in the SAM of *bop1-3 bop2-1* double mutants (Fig. 5). These results suggest that *PNY* controls flowering at least partially through repression of *BOP* gene expression to allow *FD* mRNA to increase in the meristem.

Taken together, these data indicate that the activity of the FT pathway during photoperiodic induction of flowering requires repression of *BOP* genes by *PNY*.

DISCUSSION

We performed a sensitized mutant screen to identify genes required for FT signaling during photoperiodic
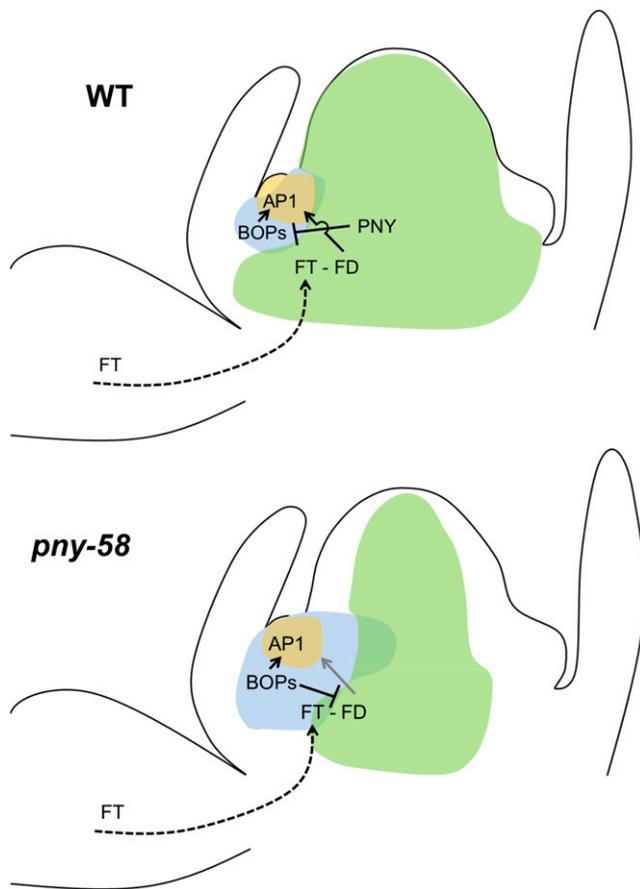
Figure 6. Model explaining the spatial regulation of flowering-related genes by *PNY* and *BOP1/2*. It has been suggested that FT is delivered from the phloem to the proximity of the SAM (dashed line; Yoo et al., 2013). Once FT is in the shoot meristem, it is supposed to interact with FD to activate the transcription of *AP1* (yellow shade). After the floral induction, *BOP1/2* activate the transcription of *AP1* mRNA in the FM. We showed that PNY directly represses *BOP1/2* expression (blue shade) in the shoot meristem, so that, in the absence of *PNY* (*pny-58*, bottom), *BOP1/2* pattern of expression becomes broader. We also found that *BOP1/2* repress *FD* expression before floral transition. Thus, the ectopic expression of *BOP1/2* in *pny* mutants leads to the reduction of the expression domain of *FD* mRNA (green shade) in the shoot meristem. Consequently, FT-FD complex formation might be impaired (gray arrow) and the transcriptional activation of *AP1* mRNA reduced.

flowering. Among all of the mutations recovered in this screen, a novel allele of the homeobox gene *PNY* caused the strongest delay in flowering. This *pny-58* allele delayed flowering both in the *pGAS1::FT ft-10 tsf-1* background used for the screen and in Col-0. Expression and genetic analyses indicated that the late flowering of *pny* mutants was caused by ectopic expression of *BOP1* and *BOP2* in the shoot meristem during vegetative development. Thus, the repression of expression of *BOP* genes is a major aspect of the contribution of *PNY* to flowering time control. This conclusion is in agreement with previous reports that repression of *BOP* genes by PNY is necessary for wild-type inflorescence development because ectopic *BOP* gene expression

causes abnormalities such as short internodes and reduced apical dominance (Norberg et al., 2005; Ha et al., 2007; Khan et al., 2012a, 2012b). Consistent with *BOP* repression being a fundamental function of PNY, we found that PNY binds directly to the promoters of both *BOP* genes. In the meristems of *pny* mutants or *bop1-6d* plants carrying a gain-of-function allele of *BOP1*, *FD* mRNA was strongly reduced, and this likely contributed to the reduced responsiveness to FT. We propose that restriction of *BOP* expression to the proximal regions of lateral organs, particularly its exclusion from the shoot meristem by PNY, is required for wild-type levels of *FD* expression and thus efficient floral induction in response to FT (Fig. 6).

Significance of Defining Organ Boundaries for FT Signaling and *FD* Expression

In plant meristems, lateral organ boundaries separate the meristematic zone containing undifferentiated cells from the lateral organs containing differentiated cells (Rast and Simon, 2008; Khan et al., 2014). The *BOP1* and *BOP2* genes are expressed at the base of lateral organs, adjacent to the boundary (Ha et al., 2004; Hepworth et al., 2005; Norberg et al., 2005). They help define the boundary region by repressing homeobox genes, which maintain the meristematic region, by directly activating *ASYMMETRIC LEAVES2* and other genes that specify the boundary (Ha et al., 2007; Jun et al., 2010). We observed that, in *pny* mutants, the *BOP* genes are ectopically expressed in the vegetative meristem, as was previously described for older inflorescence meristems (Norberg et al., 2005; Ha et al., 2007; Khan et al., 2012a, 2012b). Thus, in wild-type plants during vegetative development, PNY contributes to positioning of the boundary between the vegetative meristem and leaves by repressing *BOP* gene expression in the meristem. Indeed, we observed that, in the absence of functional *PNY* (*pny-58*), *BOP2* expression becomes broader in the meristem. Similarly, Khan et al. (2015) found that the *BOP1* spatial pattern of expression was enlarged in the inflorescence meristem of *pny pnf*. This restriction of *BOP* expression and proper localization of the boundary is required for correct timing of the floral transition, because *pny* mutants are late flowering, and this is suppressed in the *pny bop1 bop2* triple mutant (Fig. 3; Supplemental Fig. S7). The sensitized screen used to identify the *pny-58* mutation illustrated the importance of *PNY* and the *BOP* genes downstream of FT in the photoperiodic flowering pathway, as previously shown by the capacity of *pny pnf* double mutants to suppress the early-flowering phenotype caused by *35S::FT* (Kanrar et al., 2008).

At the meristem, FT is proposed to activate downstream genes by directly interacting with the bZIP FD transcription factor (Abe et al., 2005; Wigge et al., 2005). This relationship between FT-related proteins and FD is highly conserved in higher plants, having also been observed in rice and tomato (*Solanum lycopersicum*; Pnueli et al., 2001; Taoka et al., 2011). We found that the

spatial pattern of expression of *FD* in the SAM is regulated by the *PNY*, *BOP1*, and *BOP2* genes. Ectopic *BOP* gene expression in the *pny* mutant or the gain-of-function *bop1-6d* mutation strongly reduced *FD* transcription (Fig. 5). Whether this repression is due to direct recruitment of BOP proteins to the *FD* gene or an indirect effect of BOP proteins, for example, by activating transcription of boundary genes, remains unclear. Nevertheless, the reduction in *FD* mRNA likely explains the impaired sensitivity of the meristem to FT. Consistent with this idea, *LFY* and *AP1* mRNA levels were reduced in *GAS1::FT ft-10 tsf-1 pny-58* (*lgf58*) plants as observed for *GAS1::FT fd-3* and in *bop1-6d* mutants (Fig. 4; Supplemental Figs. S1 and S8). These results demonstrate that ectopic expression of *BOP* genes in the vegetative meristem reduces *AP1* and *LFY* expression during the early stages of floral transition, as expected for plants with reduced FD activity, although later in the floral primordial, BOP proteins have a direct role in the activation of *AP1* (Karim et al., 2009; Xu et al., 2010). Surprisingly, the expression levels of *LFY* were reduced during flower development in the *bop1 bop2* double mutant compared with wild-type plants (Supplemental Fig. S8; Karim et al., 2009). We interpret these data as indicating a dual role for BOP1/2 in floral development. They might act as transcriptional repressors of *LFY* and *AP1* during the early stages of floral transition (probably mediated through *FD*) and promote the expression of these two genes during floral development.

The finding that ectopic expression of BOP function represses *FD* in the meristem suggests that, in wild-type plants, *BOP* gene expression in the boundary region of lateral organs might also repress *FD*, thus reducing its expression in lateral organs and restricting it to the meristem. Interestingly, *FD* expression is excluded from a strip of cells adjacent to lateral organs that might represent the boundary domain (Fig. 5B; Wigge et al., 2005), although higher resolution analysis allowing direct comparison of boundary gene expression with *FD* will be required to test this suggestion. In response to FT signaling, downstream genes are expressed in specific spatial domains of the meristem. Spatial patterning of *FD* expression in the apex may impose spatial constraints on FT signaling by ensuring, for example, that activation of the FT pathway does not occur in boundary regions.

Genetic and Molecular Interactions between PNY and Other Homeodomain Transcription Factors in the Regulation of Flowering

PNY is a member of the TALE homeodomain transcription factor family. These proteins are divided into two classes, referred to as KNOX and BELL. PNY is a member of the BELL class and interacts in the meristem with KNOX proteins, particularly BP and SHOOT MERISTEMLESS, to form heterodimers that regulate transcription. PNF and ARABIDOPSIS THALIANA

HOMEOBOX1 (ATH1) are other BELL class proteins expressed in the meristem that have been implicated in flowering-time control (Smith et al., 2004; Proveniers et al., 2007). TALE transcription factors were shown to directly regulate genes encoding components of hormonal pathways or other transcription factors (Bolduc et al., 2012; Arnaud and Pautot, 2014). We demonstrate that PNY, presumably acting as a heterodimer with KNOX proteins expressed in the meristem, acts directly to repress genes encoding the transcriptional coactivators *BOP1* and *BOP2*.

ATH1 and KNAT6, a KNOX class protein, are expressed at lateral organ boundaries during inflorescence development, where their activation requires *BOP1/2*. During vegetative development, *ATH1* is expressed in the SAM and acts as a floral repressor. A recent study reported that BOP1 regulates the expression of *ATH1* by directly binding to its promoter (Khan et al., 2015). Therefore, the ectopic expression of BOP1/2 in the meristem of *pny* mutants might increase *ATH1* expression, contributing to the late-flowering phenotype. *ATH1* delays flowering at least partially by activating expression of the floral repressor *FLOWERING LOCUS C* (*FLC*) in the SAM. FLC represses *FD* by directly binding to its promoter (Searle et al., 2006). Thus, the repression of *FD* by *BOP1/2* could at least partially be due to increased ATH1 activity, leading to misexpression of *FLC* mRNA in the SAM (Proveniers et al., 2007). Alternatively, BOP1/2 might interact directly with the promoter of *FD*. Further studies must be done to discriminate between these possible scenarios.

PNY and the related BELL protein PNF are genetically redundant in the promotion of flowering. Nevertheless, *pny-58* was clearly late flowering in the single mutant, as described for other *pny* alleles named *blr* (Byrne et al., 2003). The *pny pnf* double mutant did not flower in any environmental condition tested and was assumed to be impaired in the competence to flower (Smith et al., 2004). Genetic and molecular analyses of the double mutant indicated that expression of *LFY* and *AP1* was strongly reduced in the inflorescence apices of these plants, but *FT* expression in leaves was unaffected (Kanrar et al., 2008). The conclusion that PNY PNF acts between FT and *LFY* was supported by the observation that *pny pnf 35S:LFY* plants produced flowers, but *pny pnf 35S:FT* plants did not (Kanrar et al., 2008). These results are in agreement with our observation that a primary effect of *pny* on flowering is reduction of *FD* mRNA, which is required for FT to promote flowering. Similarly, Lal et al. (2011) described a reduction in *SPL4* and *SPL5* expression in *pny pnf* apices, and activation of both of these genes at the shoot meristem is dependent on FT and FD (Torti et al., 2012). However, in contrast to our data, Kanrar et al. (2008) found that *FD* mRNA was present in the meristem of *pny pnf* plants at levels similar to those found in the wild type; therefore, the mechanism by which FT activity was impaired by *pny pnf* was unclear. This discrepancy with our data might be due to the age of the plants examined, as we studied *pny* mutants during vegetative development just prior

to floral induction and found a clear decrease in *FD* mRNA likely due to ectopic *BOP1/2* expression, whereas Kanrar et al. (2008) examined the inflorescence meristem of plants 20 d after floral induction had occurred in the wild-type controls. In support of our data, Jaeger et al. (2013) also reported a reduction of *FD* mRNA levels in *pny pnf* plants grown under inductive LDs, and we found that *FD* was strongly repressed in *bop1-6d* plants that express *BOP1* in the meristem. Therefore, taken together, the data suggest that flowering is delayed in *pny* and *pny pnf* mutants, at least partially, by reducing FT signaling, and our data indicate that this occurs due to reduced *FD* expression in the vegetative meristem caused by ectopic expression of *BOP1/2*, are directly repressed in wild-type plants by PNY (Fig. 6).

MATERIALS AND METHODS

Plant Materials and Growth Conditions

The wild type was the Col-0 ecotype of Arabidopsis (*Arabidopsis thaliana*). The transgenic plants p*GAS1::FT*, p*GAS1::FT ft-10 tsf-1*, and p*SOC1::SOC1:GFP soc1-2* were previously described in Jang et al. (2009) and Immink et al. (2012). The mutant alleles used were *pny-40126* (Smith and Hake, 2003), *bop1-3 bop2-1* (Hepworth et al., 2005), *fd-3* (Abe et al., 2005), *soc1-2* (Lee et al., 2000), and *ft-10 tsf-1 soc1-2* (Torti et al., 2012). The activation-tagged overexpressing line *bop1-6D* was described in Norberg et al. (2005). Plants were grown in climatic chambers under LD (16-h light/8-h dark) or SD (8-h light/16-h dark) conditions with a light intensity of 150 mmol m^{-2} s^{-1}, 21°C, and 70% relative humidity.

Molecular Cloning of pPNY::Venus:PNY

Cloning of locus *PNY* was based on polymerase incomplete primer extension (PIPE; Klock and Lesley, 2009) with modifications for large fragments and multiple inserts. All PCR amplifications were done with Phusion Enzyme (New England BioLabs) following the manufacturer's recommendations. Amplification of the *PNY* coding sequence was done from genomic DNA covering from the 5′-untranslated region (5UTR) until the 3UTR (primers A1-F/A2-R), obtaining a PCR product of 3.5 kb. The promoter was amplified from −5,553 region until 78 nucleotides of exon 1 (primers A3-F/A4-F) obtaining a PCR product of 5.7 kb. PCR products were independently cloned into pDONR201 (Invitrogen) by BP reaction generating constructs csPNY-pENTR201 and pPNY-pENTR201, respectively. Insertion of the sequence of fluorescent protein Venus (Nagai et al., 2002; Heisler et al., 2005) at the amino terminus was done by amplifying three different PCR elements adding overlap sequences among them: *I-PIPE-1* (Venus), *I-PIPE-2* (coding sequence PNY), and *vector-PIPE* (promoter PNY-pENTR201). Elaboration of *I-PIPE-1* was done by amplifying Venus and adding a linker of nine Ala to exon1 (primers A5-F/A6-R) obtaining a product of 772 nucleotides. Generation of *I-PIPE-2* was done using csPNY-pENTR201 as template, producing a PCR fragment of 3.3 kb containing the region from exon1 until 3UTR (primers A7-F/A8-R). Finally, *vector-PIPE* was generated using as template pPNY-pENTR201, obtaining a PCR fragment of 7.8 kb (primers A9-F/A10-R) comprising promoter-5UTR plus pENTR201 backbone. For the assembly of the different fragments, equimolar amounts of each *I-PIPE* element were mixed while keeping a ratio of 1:10 to vector-PIPE. The mixture was cloned into chemical competent DH5-α cells. The final construct (11.8 kb) was verified by digestion analysis and sequencing. Subsequently, the construct was cloned into the binary vector pEarleyGate301 (Earley et al., 2006) by LR reaction and transformed into *Agrobacterium tumefaciens* GV3101 cells. *pny-40126* plants were transformed by the floral-dip method (Clough and Bent, 1998). The list of primers used for the molecular cloning can be found in the Supplemental Table S2.

Mutagenesis and Genetic Screen

Approximately 10,000 seeds (200 mg) of p*GAS1::FT ft-10 tsf-1* were wrapped in miracloth and imbibed for 14 h in 50 mL of 0.1% (w/v) KCl (50 mg of KCl in 50 mL of dH$_2$O) at 4°C on a shaker. Then, the seeds were treated with 30 mM EMS for 12 h. After the treatment, the seeds were washed twice with 100 mL of 100 mM sodium thiosulfate followed by two additional washes with 500 mL of water. The seeds were transferred to a flask containing 2 L of water and distributed in 200 pots by pipetting (50 seeds/pot). M1 generation was grown in a greenhouse under LD conditions. M2 seeds from each pot were harvested together and treated as a pool. Approximately 500 M2 seeds from each pool were used for the genetic screen. The screening of the M2 seeds was performed in climatic chambers under SDs. Mutants showing late flowering compared with p*GAS1::FT ft-10 tsf-1* (*lgf* mutants) were selected, and the phenotypes were confirmed in the M3 generation.

Flowering Time Measurements

Flowering time was scored as the number of leaves at bolting. The number of rosette leaves was determined when the shoot reached approximately 0.5-cm length. The cauline leaf number was defined when the shoot was totally elongated. At least 10 individual plants were scored by genotype. All experiments were independently repeated at least twice.

Resequencing and Mapping Strategy

lgf58 homozygous mutant was crossed with p*GAS1::FT ft-10 tsf-1* to generate the BC1F2 mapping population. A total of 174 late-flowering mutants out of 566 F2 plants were selected. One leaf sample of each was harvested and pooled. Leaf material from the original p*GAS1::FT ft-10 tsf-1* parental was also harvested. Genomic DNA (gDNA) from 1 g of the pooled and the p*GAS1::FT ft-10 tsf-1* leaf material was extracted using a DNeasy Plant Maxi Kit (Qiagen). Four micrograms of gDNA was sent to the Cologne Center of Genomics (Cologne, Germany) for sequencing. Sequencing was performed on an Illumina HiSeq2000 instrument. Up to four independent gDNA samples (i.e. p*GAS1::FT ft-10 tsf-1* and various *lgf* mutants, including *lgf58*) were resequenced in a single HiSeq2000 flow cell lane with a read length of 100 bp (paired end) by using barcoding (multiplexing). After sequencing and applying the quality controls, we obtained a total of 109,948,920 reads from p*GAS::FT ft-10 tsf-1* and 87,972,438 reads from *lgf58* plants. A total of 101,934,960 (92%) reads from p*GAS::FT ft-10 tsf-1* and 85,609,714 (97%) reads from *lgf58* were aligned to the reference sequence TAIR10 (Arabidopsis Genome, 2000) by applying SHORE (Schneeberger et al., 2009b) and GenomeMapper (Schneeberger et al., 2009a), representing an average coverage of 73× and 57× the respective resequenced genome (p*GAS::FT ft-10 tsf-1* and *lgf58* population). Before identifying single nucleotide polymorphisms (SNPs) from the alignment of the pooled *lgf58* plants short read data, an SNP analysis of p*GAS::FT ft-10 tsf-1* was applied to identify all fixed SNPs of this pool. After removing these SNPs from the SNP analysis of *LGF58*, we obtained a total of 20,137 putative differences from the reference sequence. Of those, 1,174 were further removed as they were located in the mitochondria and chloroplast genome. From the remaining 18,963 putative differences, 2,212 revealed the canonical EMS mutation (G/C:A/T). From those, we obtained a final set of 137 mutations by relaxed filtering for reliable mutations (at least a SHORE quality score of 25 and a minimum allele frequency of 0.7 for the mutated allele). The list of top candidates can be found in Supplemental Table S1. Short reads are available through the European Nucleotide Archive under accession number PRJEB10593.

Protein Extraction and Immunoblotting Assays

Total protein was extracted from inflorescences, ground in liquid nitrogen and homogenized in denaturing buffer (100 mM Tris-HCl [pH 7.5], SDS 3%, 10 mM dithiothreitol, and 1% protein inhibitor), mixed by vortexing, and rotated for 10 min at 4°C. Cell debris was removed by centrifugation at 14,500 rpm for 10 min at 4°C. Proteins were quantified by the bicinchoninic acid method, and 30 μg of proteins was loaded in a gel preceded by boiling for 5 min. Anti-rabbit GFP antibody (Abcam ab290) was used for the western blot. The blot was incubated with SuperSignal Femto West Substrate (Thermo Fisher Scientific) following the manufacturer's protocol and detected with a LAS-4000 Mini-image analyzer (Fujifilm). Coomassie Brilliant Blue was used as the loading control.

ChIP and qPCR

ChIP was performed as previously described (Andrés et al., 2014; Mateos et al., 2015). GFP antibody from Abcam (ab290) was used to immunoprecipitate the chromatin. Inflorescences (containing flowers until stage 13) of

approximately 4-week-old p*PNY::Venus:PNY* and *pny-40126* plants grown under LD were collected at zeitgeber time 3 for the ChIP assays. The percentage of input method was used for data normalization (Haring et al., 2007). qPCR values obtained from the immunoprecipitated samples were divided by the qPCR values of a 1:10^2 dilution of the input sample. For validation of the PNY binding to *BOP1* and *BOP2*, several pair of primers spanning the *BOP1* and *BOP2* promoters were tested (Supplemental Table S2). Two biological replicates were performed for each ChIP assay. Only one of the replicates is shown.

qPCR Methods for RNA Expression Analysis and Genotyping of *pny-58*

RNA expression analyses were performed as described in Andrés et al. (2014). Total RNA was extracted from plant tissue by using the RNeasy Plant Mini Kit (Qiagen) and treated with DNA-free DNase (Ambion) to remove residual genomic DNA. The RNA was then quantified by using the Nanodrop ND-1000. One microgram of total RNA was used for RT (Superscript II; Invitrogen). Levels of mRNA were quantified by qPCR in a LightCycler 480 instrument (Roche) using the *PEROXIN4* gene (*AT5G25760*) as a standard. Three biological replicates were performed for each RT-qPCR assay. The average of the three replicates is shown. The list of primers used for expression analyses can be found in Supplemental Table S2. Graphs were obtained from three independent technical replicates, although all RT-qPCRs were repeated at least twice and showed identical results.

Genotyping of the mutant allele *pny-58* was performed by high-resolution melting (Wittwer et al., 2003). *pny-58* allele carried a single nucleotide change (C > T). Primers flanking this mutation (K617 and K618; Supplemental Table S2) were used to amplify (by PCR) a 79-bp amplicon from gDNA extracted from leaf material (Plant DNeasy Kit; Qiagen). The PCR products were diluted five times in water. Three microliters of the PCR product dilutions was used as a template for the qPCR in a LightCycler 480 instrument (Roche). Primers K617 and K618 were used for the amplification. The PCR conditions were as follows: 95°C for 3 min (pre-incubation) and 22 cycles of 95°C for 20 s, 60°C for 20 s, and 72°C for 20 s. For the melting curve generation, the temperature was increased from 65°C to 97°C (ramp rate 0.11°C/s and 5 acquisitions/°C). The mutant and wild-type alleles could be differentiated by analyzing the melting peaks. The *pny-58* and wild-type alleles produced a melting peak at 77.66°C ± 0.03°C and 78.33°C ± 0.03°C, respectively.

In Situ Hybridization and Microscopy Techniques

In situ hybridizations were performed as described in Torti et al. (2012). The *FD* probe was synthesized as described in Searle et al. (2006). The list of primers used to generate the other probes can be found in Supplemental Table S2. For Venus:PNY visualization in shoot meristems, a method described previously (Wang et al., 2014) was used, with small modifications. Shoot apices were collected and placed on ice-cold 2.5% paraformaldehyde (PFA; Sigma-Aldrich) prepared in phosphate-buffered saline at pH 7.0. Samples were vacuum infiltrated for 30 min, transferred to fresh 2.5% PFA, and stored at 4°C overnight. The second day, the samples were incubated for 30 min in 1% PFA supplemented with 10%, 20%, and 30% Suc. Then, samples were embedded in OCT (Sakura Finetek) at −20°C. Sections of 35 μm were made using a cryotome (Frigocut 2800; Reichert Jung). Sections containing a visible meristem were selected and mounted with ProLong Diamond Antifade (Invitrogen). The shoot meristems were imaged by confocal laser scanning microscopy (Zeiss LSM780). The confocal laser scanning microscopy settings were optimized for the visualization of Venus fluorescent proteins (laser wavelength, 514 nm; detection wavelength, 517–569 nm).

Statistical Analysis

All of the statistical analyses were performed by using SigmaStat 3.5 software.

Sequence data from this article can be found in the GenBank/EMBL data libraries under accession numbers AT5G02030 (PNY), AT3G57130 (BOP1), AT2G41370 (BOP2), AT1G65480 (FT), AT4G35900 (FD), AT2G45660 (SOC1), AT1G69120 (AP1), AT5G61850 (LFY), and AT1G53160 (SPL4).

Supplemental Data

The following supplemental materials are available.

Supplemental Figure S1. Phenotype of the mutants recovered in the genetic screen and characterization of *lgf58*.

Supplemental Figure S2. Scheme of the cloning-by-sequencing of the *lgf58* mutant.

Supplemental Figure S3. Phenotypical characterization of mutants carrying the *pny-58* allele.

Supplemental Figure S4. Flowering time of plants carrying mutations that suppress FT function.

Supplemental Figure S5. Functional characterization of p*PNY:Venus:PNY* transgenic plants.

Supplemental Figure S6. Effect of photoperiod on *PNY* pattern of expresson.

Supplemental Figure S7. Interaction between *PNY* and *BOP1/2* genes in flowering time control.

Supplemental Figure S8. Effect of *BOP1/2* genes on the FT-signalling pathway.

Supplemental Table S1. Candidate loci identified by SHOREmap.

Supplemental Table S2. List of primers used in this work.

LITERATURE CITED

Abe M, Kobayashi Y, Yamamoto S, Daimon Y, Yamaguchi A, Ikeda Y, Ichinoki H, Notaguchi M, Goto K, Araki T (2005) FD, a bZIP protein mediating signals from the floral pathway integrator FT at the shoot apex. Science **309:** 1052–1056

Andrés F, Coupland G (2012) The genetic basis of flowering responses to seasonal cues. Nat Rev Genet **13:** 627–639

Andrés F, Porri A, Torti S, Mateos J, Romera-Branchat M, García-Martínez JL, Fornara F, Gregis V, Kater MM, Coupland G (2014) SHORT VEGETATIVE PHASE reduces gibberellin biosynthesis at the Arabidopsis shoot apex to regulate the floral transition. Proc Natl Acad Sci USA **111:** E2760–E2769

Arabidopsis Genome I; Arabidopsis Genome Initiative (2000) Analysis of the genome sequence of the flowering plant Arabidopsis thaliana. Nature **408:** 796–815

Arnaud N, Pautot V (2014) Ring the BELL and tie the KNOX: roles for TALEs in gynoecium development. Front Plant Sci **5:** 93

Bao X, Franks RG, Levin JZ, Liu Z (2004) Repression of *AGAMOUS* by *BELLRINGER* in floral and inflorescence meristems. Plant Cell **16:** 1478–1489

Bolduc N, Yilmaz A, Mejia-Guerra MK, Morohashi K, O'Connor D, Grotewold E, Hake S (2012) Unraveling the KNOTTED1 regulatory network in maize meristems. Genes Dev **26:** 1685–1690

Bowman JL, Eshed Y (2000) Formation and maintenance of the shoot apical meristem. Trends Plant Sci **5:** 110–115

Byrne ME, Groover AT, Fontana JR, Martienssen RA (2003) Phyllotactic pattern and stem cell fate are determined by the Arabidopsis homeobox gene BELLRINGER. Development **130:** 3941–3950

Clough SJ, Bent AF (1998) Floral dip: a simplified method for Agrobacterium-mediated transformation of Arabidopsis thaliana. Plant J **16:** 735–743

Corbesier L, Vincent C, Jang S, Fornara F, Fan Q, Searle I, Giakountis A, Farrona S, Gissot L, Turnbull C, et al (2007) FT protein movement contributes to long-distance signaling in floral induction of Arabidopsis. Science **316:** 1030–1033

Couzigou JM, Zhukov V, Mondy S, Abu el Heba G, Cosson V, Ellis TH, Ambrose M, Wen J, Tadege M, Tikhonovich I, et al (2012) *NODULE ROOT* and *COCHLEATA* maintain nodule development and are legume

orthologs of Arabidopsis *BLADE-ON-PETIOLE* genes. Plant Cell 24: 4498–4510

Earley KW, Haag JR, Pontes O, Opper K, Juehne T, Song K, Pikaard CS (2006) Gateway-compatible vectors for plant functional genomics and proteomics. Plant J 45: 616–629

Fowler S, Lee K, Onouchi H, Samach A, Richardson K, Morris B, Coupland G, Putterill J (1999) GIGANTEA: a circadian clock-controlled gene that regulates photoperiodic flowering in Arabidopsis and encodes a protein with several possible membrane-spanning domains. EMBO J 18: 4679–4688

Ha CM, Jun JH, Nam HG, Fletcher JC (2004) BLADE-ON-PETIOLE1 encodes a BTB/POZ domain protein required for leaf morphogenesis in Arabidopsis thaliana. Plant Cell Physiol 45: 1361–1370

Ha CM, Jun JH, Nam HG, Fletcher JC (2007) *BLADE-ON-PETIOLE 1* and 2 control *Arabidopsis* lateral organ fate through regulation of LOB domain and adaxial-abaxial polarity genes. Plant Cell 19: 1809–1825

Hamant O, Pautot V (2010) Plant development: a TALE story. C R Biol 333: 371–381

Haring M, Offermann S, Danker T, Horst I, Peterhansel C, Stam M (2007) Chromatin immunoprecipitation: optimization, quantitative analysis and data normalization. Plant Methods 3: 11

Hartwig B, James GV, Konrad K, Schneeberger K, Turck F (2012) Fast isogenic mapping-by-sequencing of ethyl methanesulfonate-induced mutant bulks. Plant Physiol 160: 591–600

Hay A, Tsiantis M (2010) KNOX genes: versatile regulators of plant development and diversity. Development 137: 3153–3165

Heisler MG, Ohno C, Das P, Sieber P, Reddy GV, Long JA, Meyerowitz EM (2005) Patterns of auxin transport and gene expression during primordium development revealed by live imaging of the Arabidopsis inflorescence meristem. Curr Biol 15: 1899–1911

Hepworth SR, Zhang Y, McKim S, Li X, Haughn GW (2005) BLADE-ON-PETIOLE-dependent signaling controls leaf and floral patterning in *Arabidopsis*. Plant Cell 17: 1434–1448

Immink RG, Posé D, Ferrario S, Ott F, Kaufmann K, Valentim FL, de Folter S, van der Wal F, van Dijk AD, Schmid M, et al (2012) Characterization of SOC1's central role in flowering by the identification of its upstream and downstream regulators. Plant Physiol 160: 433–449

Jaeger KE, Pullen N, Lamzin S, Morris RJ, Wigge PA (2013) Interlocking feedback loops govern the dynamic behavior of the floral transition in *Arabidopsis*. Plant Cell 25: 820–833

Jaeger KE, Wigge PA (2007) FT protein acts as a long-range signal in Arabidopsis. Curr Biol 17: 1050–1054

Jang S, Torti S, Coupland G (2009) Genetic and spatial interactions between FT, TSF and SVP during the early stages of floral induction in Arabidopsis. Plant J 60: 614–625

Jun JH, Ha CM, Fletcher JC (2010) BLADE-ON-PETIOLE1 coordinates organ determinacy and axial polarity in *Arabidopsis* by directly activating ASYMMETRIC LEAVES2. Plant Cell 22: 62–76

Jung JH, Ju Y, Seo PJ, Lee JH, Park CM (2012) The SOC1-SPL module integrates photoperiod and gibberellic acid signals to control flowering time in Arabidopsis. Plant J 69: 577–588

Kanrar S, Bhattacharya M, Arthur B, Courtier J, Smith HM (2008) Regulatory networks that function to specify flower meristems require the function of homeobox genes PENNYWISE and POUND-FOOLISH in Arabidopsis. Plant J 54: 924–937

Kardailsky I, Shukla VK, Ahn JH, Dagenais N, Christensen SK, Nguyen JT, Chory J, Harrison MJ, Weigel D (1999) Activation tagging of the floral inducer FT. Science 286: 1962–1965

Karim MR, Hirota A, Kwiatkowska D, Tasaka M, Aida M (2009) A role for *Arabidopsis PUCHI* in floral meristem identity and bract suppression. Plant Cell 21: 1360–1372

Kaufmann K, Wellmer F, Muiño JM, Ferrier T, Wuest SE, Kumar V, Serrano-Mislata A, Madueño F, Krajewski P, Meyerowitz EM, et al (2010) Orchestration of floral initiation by APETALA1. Science 328: 85–89

Khan M, Ragni L, Tabb P, Salasini BC, Chatfield S, Datla R, Lock J, Kuai X, Després C, Proveniers M, et al (2015) Repression of lateral organ boundary genes by PENNYWISE and POUND-FOOLISH is essential for meristem maintenance and flowering in Arabidopsis. Plant Physiol 169: 2166–2186

Khan M, Tabb P, Hepworth SR (2012a) BLADE-ON-PETIOLE1 and 2 regulate Arabidopsis inflorescence architecture in conjunction with homeobox genes KNAT6 and ATH1. Plant Signal Behav 7: 788–792

Khan M, Xu H, Hepworth SR (2014) BLADE-ON-PETIOLE genes: setting boundaries in development and defense. Plant Sci 215-216: 157–171

Khan M, Xu M, Murmu J, Tabb P, Liu Y, Storey K, McKim SM, Douglas CJ, Hepworth SR (2012b) Antagonistic interaction of BLADE-ON-PETIOLE1 and 2 with BREVIPEDICELLUS and PENNYWISE regulates Arabidopsis inflorescence architecture. Plant Physiol 158: 946–960

Klock HE, Lesley SA (2009) The Polymerase Incomplete Primer Extension (PIPE) method applied to high-throughput cloning and site-directed mutagenesis. Methods Mol Biol 498: 91–103

Kobayashi Y, Kaya H, Goto K, Iwabuchi M, Araki T (1999) A pair of related genes with antagonistic roles in mediating flowering signals. Science 286: 1960–1962

Lal S, Pacis LB, Smith HM (2011) Regulation of the SQUAMOSA PROMOTER-BINDING PROTEIN-LIKE genes/microRNA156 module by the homeodomain proteins PENNYWISE and POUND-FOOLISH in Arabidopsis. Mol Plant 4: 1123–1132

Lee H, Suh SS, Park E, Cho E, Ahn JH, Kim SG, Lee JS, Kwon YM, Lee I (2000) The AGAMOUS-LIKE 20 MADS domain protein integrates floral inductive pathways in Arabidopsis. Genes Dev 14: 2366–2376

Lee I, Amasino RM (1995) Effect of vernalization, photoperiod, and light quality on the flowering phenotype of Arabidopsis plants containing the *FRIGIDA* gene. Plant Physiol 108: 157–162

Martinez-Zapater JM, Somerville CR (1990) Effect of light quality and vernalization on late-flowering mutants of *Arabidopsis thaliana*. Plant Physiol 92: 770–776

Mateos JL, Madrigal P, Tsuda K, Rawat V, Richter R, Romera-Branchat M, Fornara F, Schneeberger K, Krajewski P, Coupland G (2015) Combinatorial activities of SHORT VEGETATIVE PHASE and FLOWERING LOCUS C define distinct modes of flowering regulation in Arabidopsis. Genome Biol 16: 31

Mathieu J, Warthmann N, Küttner F, Schmid M (2007) Export of FT protein from phloem companion cells is sufficient for floral induction in Arabidopsis. Curr Biol 17: 1055–1060

Moon J, Lee H, Kim M, Lee I (2005) Analysis of flowering pathway integrators in Arabidopsis. Plant Cell Physiol 46: 292–299

Nagai T, Ibata K, Park ES, Kubota M, Mikoshiba K, Miyawaki A (2002) A variant of yellow fluorescent protein with fast and efficient maturation for cell-biological applications. Nat Biotechnol 20: 87–90

Nakamura Y, Andrés F, Kanehara K, Liu YC, Dörmann P, Coupland G (2014) Arabidopsis florigen FT binds to diurnally oscillating phospholipids that accelerate flowering. Nat Commun 5: 3553

Norberg M, Holmlund M, Nilsson O (2005) The BLADE ON PETIOLE genes act redundantly to control the growth and development of lateral organs. Development 132: 2203–2213

Pidkowich MS, Klenz JE, Haughn GW (1999) The making of a flower: control of floral meristem identity in *Arabidopsis*. Trends Plant Sci 4: 64–70

Pnueli L, Gutfinger T, Hareven D, Ben-Naim O, Ron N, Adir N, Lifschitz E (2001) Tomato SP-interacting proteins define a conserved signaling system that regulates shoot architecture and flowering. Plant Cell 13: 2687–2702

Proveniers M, Rutjens B, Brand M, Smeekens S (2007) The Arabidopsis TALE homeobox gene ATH1 controls floral competency through positive regulation of FLC. Plant J 52: 899–913

Ragni L, Belles-Boix E, Günl M, Pautot V (2008) Interaction of *KNAT6* and *KNAT2* with *BREVIPEDICELLUS* and *PENNYWISE* in *Arabidopsis* inflorescences. Plant Cell 20: 888–900

Rast MI, Simon R (2008) The meristem-to-organ boundary: more than an extremity of anything. Curr Opin Genet Dev 18: 287–294

Roeder AH, Ferrándiz C, Yanofsky MF (2003) The role of the REPLUMLESS homeodomain protein in patterning the Arabidopsis fruit. Curr Biol 13: 1630–1635

Romera-Branchat M, Andrés F, Coupland G (2014) Flowering responses to seasonal cues: what's new? Curr Opin Plant Biol 21: 120–127

Schmid M, Uhlenhaut NH, Godard F, Demar M, Bressan R, Weigel D, Lohmann JU (2003) Dissection of floral induction pathways using global expression analysis. Development 130: 6001–6012

Schneeberger K (2014) Using next-generation sequencing to isolate mutant genes from forward genetic screens. Nat Rev Genet 15: 662–676

Schneeberger K, Hagmann J, Ossowski S, Warthmann N, Gesing S, Kohlbacher O, Weigel D (2009a) Simultaneous alignment of short reads against multiple genomes. Genome Biol 10: R98

Schneeberger K, Ossowski S, Lanz C, Juul T, Petersen AH, Nielsen KL, Jørgensen JE, Weigel D, Andersen SU (2009b) SHOREmap:

simultaneous mapping and mutation identification by deep sequencing. Nat Methods **6:** 550–551

Searle I, He Y, Turck F, Vincent C, Fornara F, Kröber S, Amasino RA, Coupland G (2006) The transcription factor FLC confers a flowering response to vernalization by repressing meristem competence and systemic signaling in Arabidopsis. Genes Dev **20:** 898–912

Smaczniak C, Immink RG, Muiño JM, Blanvillain R, Busscher M, Busscher-Lange J, Dinh QD, Liu S, Westphal AH, Boeren S, et al (2012) Characterization of MADS-domain transcription factor complexes in Arabidopsis flower development. Proc Natl Acad Sci USA **109:** 1560–1565

Smith HM, Campbell BC, Hake S (2004) Competence to respond to floral inductive signals requires the homeobox genes PENNYWISE and POUND-FOOLISH. Curr Biol **14:** 812–817

Smith HM, Hake S (2003) The interaction of two homeobox genes, *BREVIPEDICELLUS* and *PENNYWISE*, regulates internode patterning in the Arabidopsis inflorescence. Plant Cell **15:** 1717–1727

Staneloni RJ, Rodriguez-Batiller MJ, Legisa D, Scarpin MR, Agalou A, Cerdán PD, Meijer AH, Ouwerkerk PB, Casal JJ (2009) Bell-like homeodomain selectively regulates the high-irradiance response of phytochrome A. Proc Natl Acad Sci USA **106:** 13624–13629

Suárez-López P, Wheatley K, Robson F, Onouchi H, Valverde F, Coupland G (2001) CONSTANS mediates between the circadian clock and the control of flowering in Arabidopsis. Nature **410:** 1116–1120

Sun H, Schneeberger K (2015) SHOREmap v3.0: fast and accurate identification of causal mutations from forward genetic screens. Methods Mol Biol **1284:** 381–395

Tamaki S, Matsuo S, Wong HL, Yokoi S, Shimamoto K (2007) Hd3a protein is a mobile flowering signal in rice. Science **316:** 1033–1036

Taoka K, Ohki I, Tsuji H, Furuita K, Hayashi K, Yanase T, Yamaguchi M, Nakashima C, Purwestri YA, Tamaki S, et al (2011) 14-3-3 proteins act as intracellular receptors for rice Hd3a florigen. Nature **476:** 332–335

Teper-Bamnolker P, Samach A (2005) The flowering integrator FT regulates *SEPALLATA3* and *FRUITFULL* accumulation in *Arabidopsis* leaves. Plant Cell **17:** 2661–2675

Torti S, Fornara F, Vincent C, Andrés F, Nordström K, Göbel U, Knoll D, Schoof H, Coupland G (2012) Analysis of the *Arabidopsis* shoot meristem transcriptome during floral transition identifies distinct regulatory patterns and a leucine-rich repeat protein that promotes flowering. Plant Cell **24:** 444–462

Valverde F, Mouradov A, Soppe W, Ravenscroft D, Samach A, Coupland G (2004) Photoreceptor regulation of CONSTANS protein in photoperiodic flowering. Science **303:** 1003–1006

Wang JW, Czech B, Weigel D (2009) miR156-regulated SPL transcription factors define an endogenous flowering pathway in Arabidopsis thaliana. Cell **138:** 738–749

Wang Q, Kohlen W, Rossmann S, Vernoux T, Theres K (2014) Auxin depletion from the leaf axil conditions competence for axillary meristem formation in *Arabidopsis* and tomato. Plant Cell **26:** 2068–2079

Weigel D, Alvarez J, Smyth DR, Yanofsky MF, Meyerowitz EM (1992) LEAFY controls floral meristem identity in Arabidopsis. Cell **69:** 843–859

Wigge PA, Kim MC, Jaeger KE, Busch W, Schmid M, Lohmann JU, Weigel D (2005) Integration of spatial and temporal information during floral induction in Arabidopsis. Science **309:** 1056–1059

Wilson RN, Heckman JW, Somerville CR (1992) Gibberellin is required for flowering in *Arabidopsis thaliana* under short days. Plant Physiol **100:** 403–408

Wittwer CT, Reed GH, Gundry CN, Vandersteen JG, Pryor RJ (2003) High-resolution genotyping by amplicon melting analysis using LCGreen. Clin Chem **49:** 853–860

Xu M, Hu T, McKim SM, Murmu J, Haughn GW, Hepworth SR (2010) Arabidopsis BLADE-ON-PETIOLE1 and 2 promote floral meristem fate and determinacy in a previously undefined pathway targeting APETALA1 and AGAMOUS-LIKE24. Plant J **63:** 974–989

Yamaguchi A, Kobayashi Y, Goto K, Abe M, Araki T (2005) TWIN SISTER OF FT (TSF) acts as a floral pathway integrator redundantly with FT. Plant Cell Physiol **46:** 1175–1189

Yamaguchi A, Wu MF, Yang L, Wu G, Poethig RS, Wagner D (2009) The microRNA-regulated SBP-Box transcription factor SPL3 is a direct upstream activator of LEAFY, FRUITFULL, and APETALA1. Dev Cell **17:** 268–278

Yoo SC, Chen C, Rojas M, Daimon Y, Ham BK, Araki T, Lucas WJ (2013) Phloem long-distance delivery of FLOWERING LOCUS T (FT) to the apex. Plant J **75:** 456–468

Yoo SK, Chung KS, Kim J, Lee JH, Hong SM, Yoo SJ, Yoo SY, Lee JS, Ahn JH (2005) *CONSTANS* activates *SUPPRESSOR OF OVEREXPRESSION OF CONSTANS 1* through *FLOWERING LOCUS T* to promote flowering in Arabidopsis. Plant Physiol **139:** 770–778

Yu S, Galvão VC, Zhang YC, Horrer D, Zhang TQ, Hao YH, Feng YQ, Wang S, Schmid M, Wang JW (2012) Gibberellin regulates the *Arabidopsis* floral transition through miR156-targeted SQUAMOSA PROMOTER BINDING-LIKE transcription factors. Plant Cell **24:** 3320–3332